RSC Advances

ROYAL SOCIETY OF CHEMISTRY

www.rsc.org/advances

A simple colorimetric and fluorogenic chemosensor for selective detection of Cu^{2+} ions in aqueous media

Urmiladevi Narad Yadav[a], Preeti Pant[a], Suban Kumar Sahoo[b], Ganapati Subray Shankarling[a,*]

[a]*Dyestuff Technology Department, Institute of Chemical Technology, Matunga, Mumbai 400 019, India*

[b]*Department of Applied Chemistry, SV National Institute of Technology (SVNIT), Surat-395007, India.*

*Corresponding author (Dr. GS Shankarling) E-mail addresses: gsshankarling@gmail.com, gs.shankarling@ictmumbai.edu.in Tel.: +91 2233612708; fax: +91 22 33611020.

Graphical Abstract

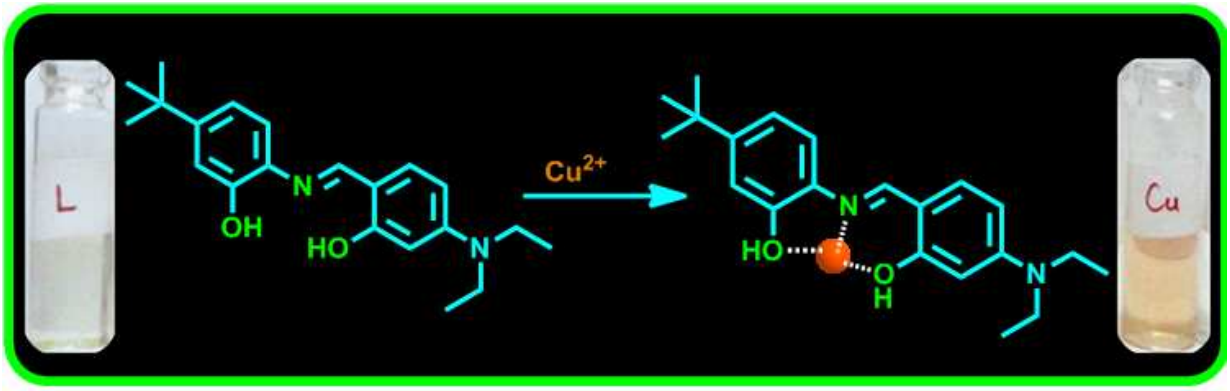

Cite this: DOI: 10.1039/c0xx00000x

www.rsc.org/xxxxxx

Paper

A novel colorimetric and fluorogenic chemosensor for selective detection of Cu^{2+} ions in mixed aqueous media

*Urmiladevi Narad Yadav[a], Preeti Pant[a], Suban Kumar Sahoo[b], Ganapati Subray Shankarling[a,]**

Received (in XXX, XXX) Xth XXXXXXXXX 20XX, Accepted Xth XXXXXXXXX 20XX

DOI: 10.1039/b000000x

A novel and easy-to-synthesize chemosensor (**L**) was developed for the selective sensing of Cu^{2+} ions in mixed aqueous medium. Sensor **L** showed both colorimetric and spectral (UV-Vis and fluorescence) responses towards Cu^{2+}, which was not affected in the presence of other surveyed metal ions (Na^{+}, Mg^{2+}, Al^{3+}, K^{+}, Ca^{2+}, Fe^{2+}, Co^{2+}, Ni^{2+}, Zn^{2+}, Ba^{2+}, Hg^{2+} and Pd^{2+}). The 1:1 binding stoichiometry between Cu^{2+} and **L** was obtained using the Job's plot and ESI-MS analysis. The binding constant (K_a) of 1.56 x 10^4 M^{-1} for **L**-Cu^{2+} complex was calculated from the Benesei-Hildebrand plot. Further, theoretical calculations were performed using the density functional theory (DFT) method to complement the experimental results.

Introduction

Metal ions play an important role in living systems as they have a striking physiological, ecological and toxicological impact on the environmental and biological systems. As a result, the detection and determination of metal ions have gained considerable attention. Among the transition metal ions, copper is an essential element for all living systems, and plays a significant role in variety of fundamental physiological processes such as respiration, antioxidant defense and iron metabolism in organisms ranging from bacteria to mammals [1]. In human, an increase in concentration of copper over normal permissible limit causes an imbalance in the cellular processes which can lead to different neurodegenerative diseases such as Alzheimer's disease [2], Wilson's disease [3], Menke's disease [4] and Indian childhood cirrhosis (ICC) [5]. In view of these detrimental effects, a suitable technique for the selective detection of Cu^{2+} is worth developing. The conventional methods used for the detection of copper ions are atomic absorption spectroscopy (AAS) [6], inductively coupled plasma emission or mass spectrometry (ICP-ES, ICP-MS) [7], total reflection X-Ray fluorimetry (TXRF) and anodic stripping voltammetry (ASV) [8], which provide good detection limits. However, these methods require high-cost analytical instrumentation and also have operational difficulties.

As an alternative to these methods, colorimetric and/or fluorescent sensors have been demonstrated to be powerful tools for the detection of copper ions. Therefore, many studies concerned with copper ions detection by colorimetric and/or fluorescent sensors containing quinolone and its derivatives [9], anthraquinone [10–13], coumarin [14–16], rhodamine [17–22], naphthalimide [23–26], BODIPY [27,28], fluorescein [29] pyrene [30,31] and other fluorophores have been reported. However, most of the copper chemosensors reported so far have disadvantages such as multi-ion detection [32], requirement of organic solvents for sensing, and interferences from other metal ions. Some of the reported receptors often require relatively tedious multi-step synthetic procedure[33]. Therefore, there is a need for the low cost and easy-to-synthesize chemosensor, which can selectively detect Cu^{2+} in aqueous medium. Recently, radical based reagent with high selectivity and sensitivity for Cu^{2+} is been reported in literature[34,35]. It provides an situ evaluation of solvated Cu^{2+} in aqueous environments. Mukhopadhyay et. al.,[36] have reported for the first time formation of a persistent radical cation of naphthalenediimide with Cu^{2+}/Fe^{3+} which exhibit panchromatic and NIR optical bands and can be used as multichannel probes.

As a part of our on-going research on analytes recognition, we have developed a novel and easy-to-make Schiff base chemosensor (**L**) (Scheme 1) for the selective detection of Cu^{2+} ions in mixed aqueous medium. Notably, the sensor **L** overcomes the drawbacks described above and exhibits unique features such as: (i) high specificity, selectivity and sensitivity towards Cu^{2+}, (ii) assays can be performed to detect Cu^{2+} from mixed aqueous media and (iii) a noticeable ratiometric spectral response and colorimetric change.

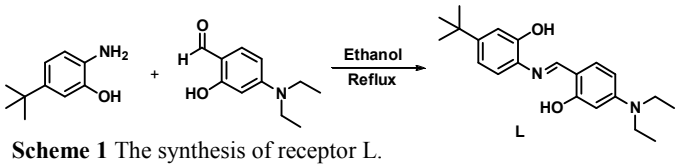

Scheme 1 The synthesis of receptor L.

Experimental Section

Materials and methods

All analytical grade chemicals and reagents were procured from SD Fine Chemical Ltd. (Mumbai, India) and were used without further purification. The reactions were monitored by thin-layered chromatography (TLC) using 0.25 mm E-Merck silica gel 60 F_{254} precoated plates, which were visualized with UV

light. ^{1}H NMR and ^{13}C NMR spectra were recorded on a 600 MHz Varian mercury plus spectrometer in DMSO-d_6 solvent. Chemical shifts were expressed in δ ppm using TMS as an internal standard. Mass spectral data were obtained with a micromass-Q-TOF (YA105) spectrometer using CH_3OH as solvent.

Synthesis of receptor L

4-(Diethylamino)salicylaldehyde (1 g, 6 mmol) and 2-amino-5-(tert-butyl)phenol (0.85 g, 5 mmol) were mixed in 10 mL methanol. Then, the reaction mass was refluxed for 5-6 hr. After completion of the reaction as indicated by TLC, the reaction solution was cooled to room temperature and the solvent was removed under reduced pressure to obtain the solid. The crude product was purified by recrystallization in methanol and dried in oven at 50°C. Yield = 1.51 g, 87%. Melting Point: 155°C; FT-IR (KBr, cm^{-1}): 3303, 3152, 3104, 2954, 2898, 1652, 1580, 1501, 1207, 1160; ^{1}H NMR (600 MHz, DMSO-d_6, ppm, Me_4Si): δ = 1.10 (s, 6H, -CH_3), 1.26 (s, 9H, -CH_3), 3.36 (q, 4H, -CH_2), 5.94 (d, J = 8.0 Hz, 1H), 6.24 (d, J = 6.0 H, 2Hz), 6.81(d, J = 6.0 H, 2Hz), 7.00 (d, J = 6.0 H, 2Hz), 7.23 (s, 1H), 7.25 (d, J = 6.0 H, 2Hz), 8.65 (s, 1H), 9.34 (s, 1H, -OH), 14.26 (s,1H, -OH); ^{13}C NMR (100 MHz, DMSO-d_6, ppm, Me_4Si):12.58, 31.35, 33.90, 43.82, 97.25, 103.54, 109.03, 115.44, 115.60, 122.74,133.65, 133.89, 141.95, 147.57, 151.54, 158.42, 165.96; HRMS *m/z* 341.2181 $(M + H)^+$, calculated *m/z* 340.46.

UV-Visible and fluorescence experiments

UV-Visible spectra was recorded on a Perkin Elmer Lamda 25 UV–VIS spectrophotometer. The fluorescence experiments were performed using Varian Cary Eclipse fluorescence spectrophotometer using freshly prepared solutions and quartz cell of 1 cm path length. The emission spectra were recorded between 430-700 nm by exciting the receptor at 425 nm. Excitation and emission slit width was kept at 5, and the data were smoothen using Savitzky-Golay smoothing filter. All the experimental parameters were kept constant throughout in order to have precision and accuracy.

All stock solutions of the metal salts (1.0×10^{-3} M) were prepared in double distilled water. Stock solution of **L** (1.0×10^{-5} M) was prepared in CH_3CN. All spectroscopic experiments were performed in CH_3CN/H_2O (9:1, v/v). Spectral titrations were carried out by taking fixed concentration of **L** directly into the cuvette and then incremental amount of $[Cu^{2+}]$ (1.0×10^{-3} M) was added by using micropipette. After each aliquot addition of Cu^{2+}, the spectra were recorded. The change in absorbance at 504 nm was plotted against cation concentrations to obtain useful results. Job's plot was plotted using equimolar concentration of **L** and Cu^{2+}. The total concentration of **L** and Cu^{2+} was kept at a constant of 1.0 X 10^{-4} M.

Calculation of fluorescence quantum yield

The fluorescence quantum yield was determined using quinine sulfate as standard with a known Φ value of 0.54 in 0.1M H_2SO_4. The quantum yield of free receptor L was calculated using the below formula[37]:

$$\Phi_s = (A_s/A_r).(f_s/f_r)(\eta_r^2/\eta_r^2).\Phi_r$$

Where, Φ_s and Φ_r are photoluminescence quantum yield of sample and reference respectively. As and Ar are the integrated intensities (area under the curve) of sample and reference spectra, respectively. The terms fr and fs represent the absorption factors for sample and reference respectively, while η is the solvent refractive index.

Results and discussion

UV-Visible absorption studies

Schiff base receptor **L** was synthesized with an excellent yield *via* a one-pot condensation of aldehyde–amine (Scheme 1), and the molecular structure was established by various spectroscopic data (Fig. S1-4). Then, the colorimetric response of receptor **L** was investigated by a series of host-guest interaction study with different metal ions (Na^+, Mg^{2+}, Al^{3+}, K^+, Ca^{2+}, Fe^{2+}, Co^{2+}, Ni^{2+}, Cu^{2+}, Zn^{2+}, Ba^{2+}, Hg^{2+}, Pd^{2+}) in CH_3CN/H_2O (9:1, v:v). On addition of Cu^{2+} ions, a naked-eye detectable color change was observed from light yellow to orange-brown (Fig. 1). No significant color change was observed with the other tested metal ions. The results clearly support the selectivity of **L** towards Cu^{2+} over the other tested metal ions.

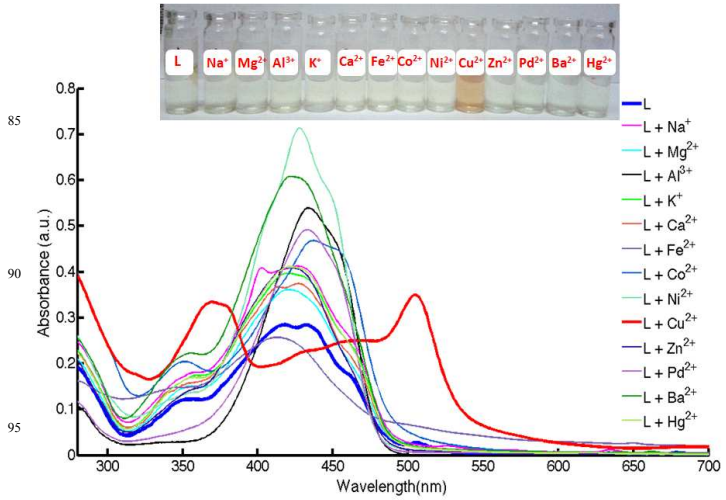

Fig. 1 UV-Visible absorption spectra of **L** (1.0 X 10^{-5}M) in the presence of 200 µL of various cations (1.0 X 10^{-3}M) in CH_3CN/H_2O (9:1, v:v).

The photophysical property of **L** was next studied by UV-Vis absorption spectroscopy (Fig. 1). UV-Vis spectrum of free receptor **L** showed a broad absorbance with maxima at 425 nm which can be accounted for overall intramolecular charge transfer (ICT). On addition of 200 µL of Cu^{2+} ions (1 x 10^{-3} M), the absorption band of **L** (1x 10^{-5} M) disappeared with the appearance of two new peaks, one with high absorption intensity centred at 504 nm and another at 365 nm. The spectral responses can be attributed to the change in structural conformation of **L** on interaction with Cu^{2+}, which mostly reflects the coordinative interaction between the lone electron pair(s) of the donor hetero-atoms (OH, N) which are conjugated to the ligand's π-system and the cation. There is an increase in conjugation of the receptor in a tightly bound complex with Cu^{2+}, resulting in planarization of

complex and red-shift. However, no such considerable change was induced by the addition of other metal ions.

Competitive binding experiment was carried out in order to examine the specificity of the receptor **L** towards Cu^{2+} ions. As shown in Fig. 2, the spectral responses and color change of the receptor **L** towards Cu^{2+} ions was not affected in presence of other interfering ions. Further, to gain an insight and to understand the recognition capability and mechanism, absorption titration experiment of **L** with Cu^{2+} was performed (Fig. 3). The spectra were recorded after successive addition of incremental amount of Cu^{2+} from 9.1 x 10^{-6} to 9.1 x 10^{-5} M (0-200 µL) to a fixed concentration of **L**. The absorbance at 504 nm increased with the formation of an isobestic point which indicates the formation of a new complex species between **L** and the added Cu^{2+}. The association constant was calculated using the linear Benesi-Hildebrand expression by plotting a graph between the measured intensity $1/(A-A_0)$ at 504 nm as a function of $1/[Cu^{2+}]$ (Fig. 3). The association constant of 1.56 x 10^4 M^{-1} was obtained by dividing the intercept with slope.

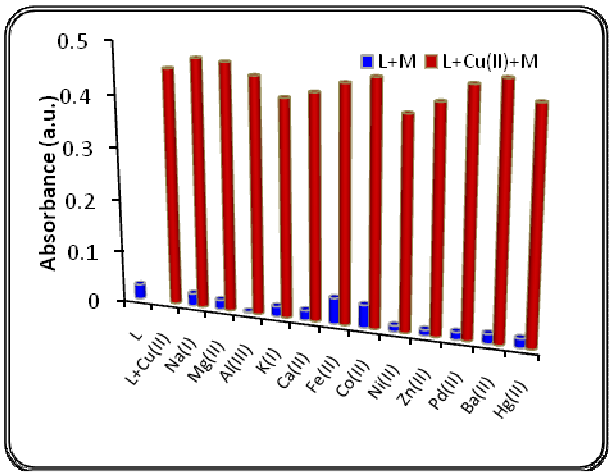

Fig. 2 Competitive binding experiments: absorbance response of L (10 µM) to Cu^{2+} in the absence and presence of competing metal ions.

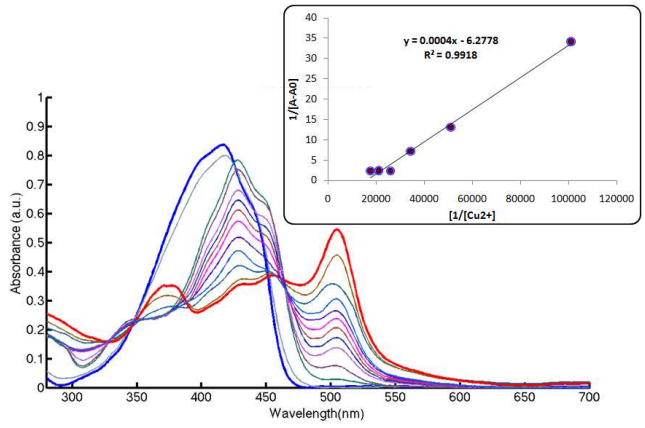

Fig. 3 UV-Visible absorption titration of L on successive addition of Cu^{2+} ions (9.1 x 10^{-6} - 9.1 x 10^{-5}M). Inset showing the Benesi-Hildebrand plot where A_0 and A stand respectively for the absorbance intensity in the absence and presence of Cu^{2+} ions.

The binding stoichiometry of the **L**-Cu^{2+} complex was determined using the continuous variations (Job's method) method (Fig. 4). When the molar fraction of **L** was 0.5, the absorbance value approached a maximum, which demonstrated the formation of a 1:1 complex between the receptor **L** and Cu^{2+}. Further, the formation of 1:1 complex was confirmed by ESI-MS which gave a prominent peak at 475.51 for $[\mathbf{L}+CuCl_2+H^+]^+$ (Fig. S5).

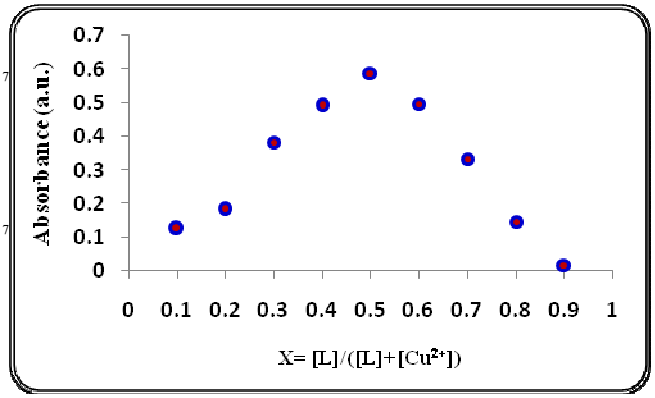

Fig. 4 Job's plot of the L-Cu^{2+} complexes in CH_3CN/H_2O (v/v = 9:1). The total concentration of L and Cu^{2+} was 1.0 X 10^{-4}M. The monitored wavelength was 505 nm.

The binding of Cu^{2+} with **L** was further supported by ^{1}H-NMR study. As shown in Fig. 5, before addition of Cu^{2+}, the receptor showed two signals at δ = 9.33 ppm and δ = 14.2 ppm accounting for the two -OH groups. The downfield value of -OH is due to the intramolecular hydrogen bonding between the imine-N atom of Schiff base with -OH group giving rise to six member transition state. On addition of Cu^{2+} ions, the intramolecular hydrogen bonding is disturbed and there is a dramatic shift in the signals as shown in the stacked NMR pictograph (Fig. 5). The aromatic protons shifted downfield indicating the influence of copper ions abrupting the electron flow in the probe. The shift in the ^{1}H NMR peaks of **L** in presence of Cu^{2+} clearly delineated that the binding occurred through the two -OH groups and imine-N atom.

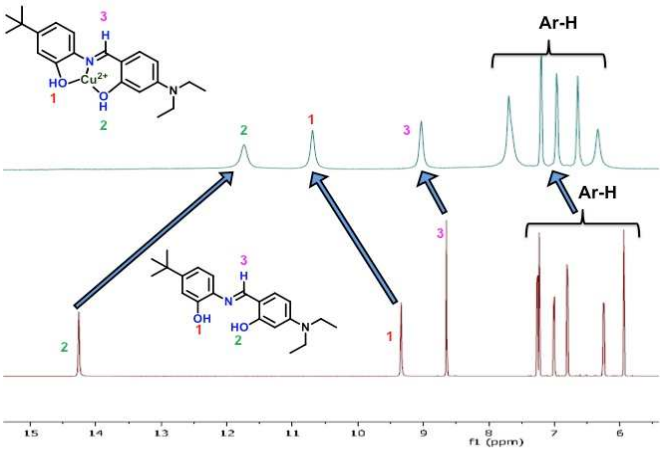

Fig. 5 ^{1}H-NMR stacked plots showing the change in the proton signal of **L** on binding with Cu^{2+} ions in DMSO-d_6.

The density functional theory (DFT) calculations by applying the B3LYP functional, and the basis sets 6-31G** (for C, H, N and O atoms) and LANL2DZ (for Cu atom) were performed in the gas phase to examine the charge transfer process occurred during the encapsulation of Cu^{2+} by receptor **L** (Fig. 6). All calculations were done by using the computational code Gaussian 09W[34]. The lowering in the interaction energy (E_{int} = E_{CuL}-E_{Cu}-E_L) of the optimized structure of **L** was observed by -353.17 kcal/mol on complexation with Cu^{2+} (Fig. 4), which indicates the formation of a stable **L**-Cu^{2+} complex with the calculated bond lengths of Cu-N (2.063 Å) and average Cu-O (2.051 Å). Further, the diagrams of highest occupied molecular orbital (HOMO) and lowest unoccupied molecular orbital (LUMO) of **L** and **L**-Cu^{2+} complex were analysed (Fig. 6). The electron density was uniformally distributed in the entire molecule of free receptor. However, in case of **L**-Cu^{2+} complex, the intramolecular charge transfer (ICT) process was observed between the receptor **L** and Cu^{2+}. Also, the band gap between the HOMO and LUMO was lowered which complemented well with the experimentally observed red-shift in the absorption band of **L** on interaction with Cu^{2+}.

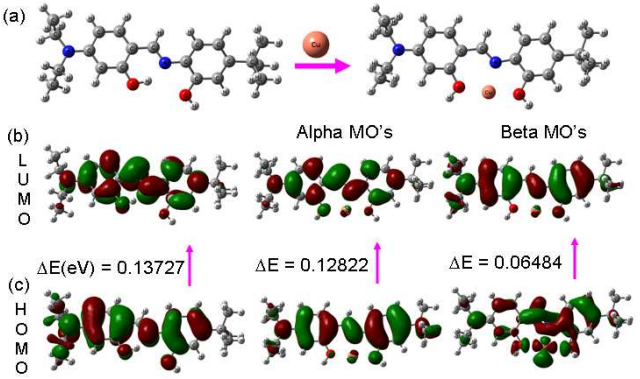

Fig. 6 DFT computed (a) optimized structure of receptor L and its complex with $Cu^{2+,}$ and the (b) LUMO and (c) HOMO diagrams of L and its L-Cu^{2+} complex.

Fluorescence studies

In good agreement with the findings form absorption study, the receptor **L** also exhibited a specific emission response towards Cu^{2+} under similar conditions (Fig. 7). The free receptor **L** emitted at 494 nm, when excited at 425 nm. Upon addition of Cu^{2+} ions, the fluorescence of **L** was selectively quenched at 494 nm due to the paramagnetic nature of Cu^{2+} that allows electron transfer from **L** to **L**-Cu^{2+} complex. The fluorescence quantum yield(Φ) of free receptor L decreased from 0.033 to 0.0009 due to complete quenching of fluorescence on binding with Cu^{2+} ion. Also, the fluorescence quenching of **L** by Cu^{2+} was visible under UV light. When the added Cu^{2+} was more than one equivalent of **L**, complete fluorescence quenching was observed due chelation-induced fluorescence quenching phenomenon. However, such fluorescence quenching was not observed in presence of other metal ions.

Next, to evaluate the response time, a time-dependent graph indicating the change in fluorescent intensity with respect to time was plotted (Fig. S6). It was observed that the emission of **L** at 494 nm quenched instantaneously but the intensity of the turn-on fluorescence at 420 nm enhanced continuously with time up to 20 min. Therefore, all the fluorescence spectra were recorded after the interval of 20 min. Further, the fluorescence titration study (Fig. 8) revealed a gradual drop in the fluorescence intensity of **L** at 494 nm and a steady rise of intensity around 420 nm on increasing the concentration of copper ions from 9.1 x 10^{-6} to 9.1 x 10^{-5} M. From the emission titration data, the limit of detection (LOD) of 1.15 x 10^{-6} M was estimated from the calibration curve (Fig. S7) and then compared with some recently reported Cu^{2+} sensors (Table 1).

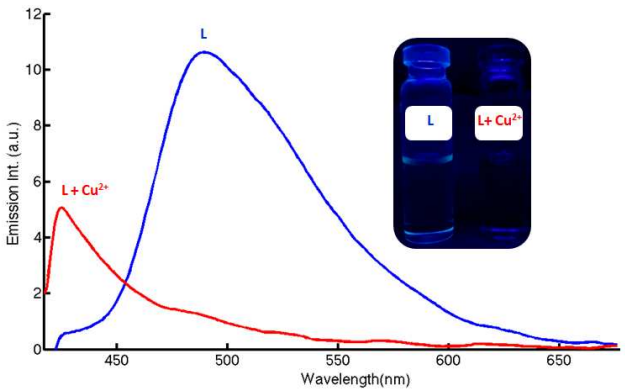

Fig. 7 Fluorescence spectra of **L** (10 μM) before and after addition of Cu^{2+} in CH_3CN/H_2O (v/v = 9:1) solution. Inset showing the color change under UV light (λex = 425 nm).

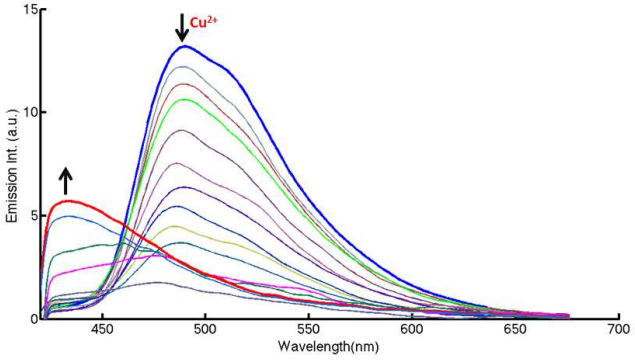

Fig. 8 Fluorescence spectral titration of **L** (10 μM) after successive addition of different concentrations of Cu^{2+} (9.1 x 10^{-6} - 9.1 x 10^{-5} M) in CH_3CN/H_2O (9:1, v/v) (λex = 425 nm).

Finally, the effect of varying pH on **L** and its **L**-Cu^{2+} complex was also studied (Fig. 9 and Fig. S8). The pH of the solution were varied by adding small amount of HCl or NaOH to HEPES (pH=7, 10mM) buffer. The emission intensity of free **L** decreased at 494 nm with the rise in the pH. In presence of Cu^{2+} ions, the emission intensity of **L** quenched at all pH but the complete quenching was observed in the physiologcal pH range of 5-10. The molecular probe **L** undergoes fluorescence quenching both with the increase in pH and increase in concentration of Cu^{2+}. The Cu^{2+} induced deprotonation of the probe might be responsible for ICT. Similarly, the pH range 5-10 was also found

to be suitable for the sensing of Cu^{2+} by **L** in the UV-Vis absorption study (Fig. 9S). These results clearly delineated the ability of **L** in effective detection of Cu^{2+} ions in biological conditions.

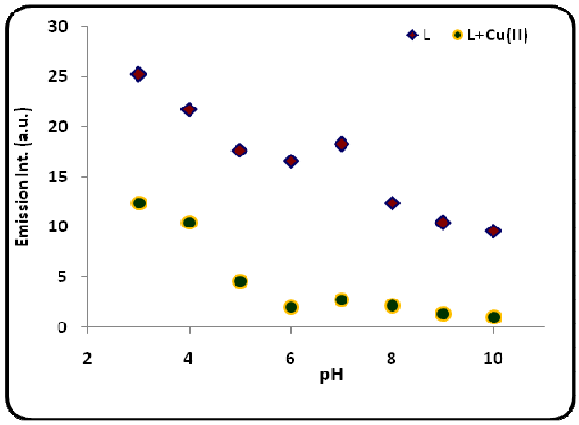

Fig. 9 Fluorescence intensity of **L** (10 μM) at different pH in the absence and presence of Cu^{2+} ions (10^{-3} M) (λex = 425 nm, λem = 494 nm).

Table 1 Comparative study of analytical performance of sensor **L** with other reported receptors.

Sr. No.	Receptors	Association Constant (K_a) (M^{-1})	Limit of Detection (M)	Ref.
1.	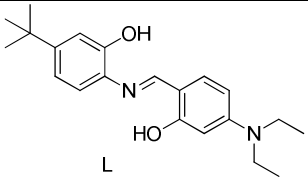 L	1.5×10^4	1.15×10^{-6}	**This work**
2.	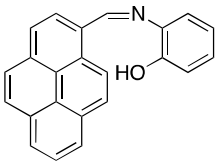	1.96×10^6	9.72×10^{-7}	38
3.	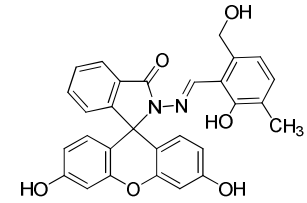	1.17×10^5	0.14×10^{-6}	39
4.	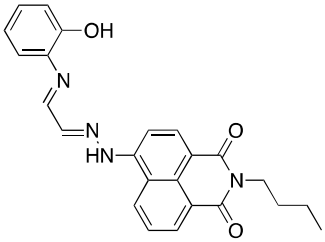	1.1×10^{10}	0.15×10^{-6}	40
5.	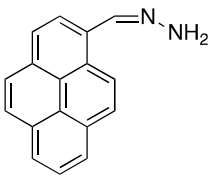	4.583×10^3	4.0×10^{-8}	41

6.	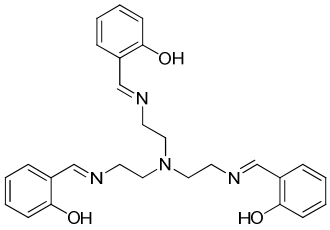	5.0118×10^4	1.5×10^{-6}	42
7.	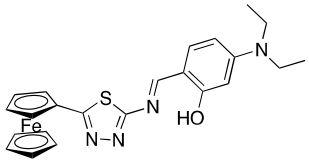	3.427×10^4	4.477×10^{-7}	43
8.	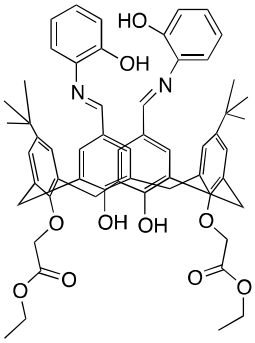	3.8×10^4	NA	44
9.	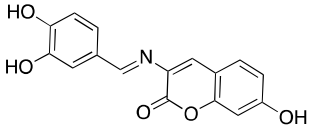	NA	1.27×10^{-4}	37
10.	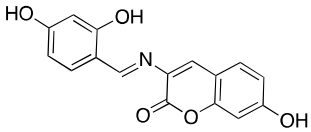	NA	1.04×10^{-4}	37

Conclusions

In summary, we have developed a simple colorimetric sensor for the selective detection of Cu^{2+} ions in mixed aqueous media. Sensor **L** showed an immediate color change from light yellow to orange-brown by forming a complex with Cu^{2+}, in 1:1 stoichiometry. The sensor showed selective dual-mode (chromogenic and fluorogenic) responses towards Cu^{2+} which made qualitative and quantitative detection possible with the detection limit down to 1.15×10^{-6} M. Importantly, this sensor can be applied in a wide pH range 5-10 and also under physiological conditions.

Acknowledgements

Authors are thankful to UGC-CAS for providing financial assistance and to the Institute of Chemical Technology (ICT), SAIF IIT-Bombay for recording FTIR, HRMS and TIFR Mumbai for ^1H and ^{13}C-NMR.

Notes and references

[a]*Dyestuff Technology Department, Institute of Chemical Technology, Matunga, Mumbai 400 019, India. Fax: +91 22 33611020; Tel: +91 2233612708; E-mail:gsshankarling@gmail.com, gs.shankarling@ictmumbai.edu.in*

[b]*Department of Applied Chemistry, SV National Institute of Technology (SVNIT), Surat-395007, India. E-mail:suban_sahoo@rediffmail.com*

† Electronic Supplementary Information (ESI) available: [details of any supplementary information available should be included here]. See DOI: 10.1039/b000000x/

1. H. Tapiero, D. M. Townsend, and K. D. Tew, *Biomed. Pharmacother.*, 2003, **57**, 386–398.
2. Y. Hung, A. Bush, and R. Cherny, *JBIC J. Biol. Inorg. Chem.*, 2010, **15**, 61–76.
3. P. C. Bull, G. R. Thomas, J. M. Rommens, J. R. Forbes, and D. W. Cox, *Nat Genet*, 1993, **5**, 327–337.
4. C. Vulpe, B. Levinson, S. Whitney, S. Packman, and J. Gitschier, *Nat Genet*, 1993, **3**, 7–13.
5. S. H. Hahn, M. S. Tanner, D. M. Danke, and W. A. Gahl, *Biochem. Mol. Med.*, 1995, **54**, 142–145.

6. A. P. S. Gonzáles, M. A. Firmino, C. S. Nomura, F. R. P. Rocha, P. V Oliveira, and I. Gaubeur, *Anal. Chim. Acta*, 2009, **636**, 198–204.

7. Y. Liu, P. Liang, and L. Guo, *Talanta*, 2005, **68**, 25–30.

8. P. Pathirathna, Y. Yang, K. Forzley, S. P. McElmurry, and P. Hashemi, *Anal. Chem.*, 2012, **84**, 6298–6302.

9. J. S. Park, S. Jeong, S. Dho, M. Lee, and C. Song, *Dye. Pigment.*, 2010, **87**, 49–54.

10. N. Kaur and S. Kumar, *Tetrahedron*, 2008, **64**, 3168–3175.

11. N. Kaur and S. Kumar, *Chem. Commun.*, 2007, 3069–3070.

12. N. Kaur and S. Kumar, *Tetrahedron Lett.*, 2008, **49**, 5067–5069.

13. S.-P. Wu, K.-J. Du, and Y.-M. Sung, *Dalt. Trans.*, 2010, **39**, 4363–4368.

14. W. Lin, L. Yuan, X. Cao, W. Tan, and Y. Feng, *European J. Org. Chem.*, 2008, **2008**, 4981–4987.

15. H. S. Jung, P. S. Kwon, J. W. Lee, J. Il Kim, C. S. Hong, J. W. Kim, S. Yan, J. Y. Lee, J. H. Lee, T. Joo, and J. S. Kim, *J. Am. Chem. Soc.*, 2009, **131**, 2008–2012.

16. A. Helal, M. H. O. Rashid, C.-H. Choi, and H.-S. Kim, *Tetrahedron*, 2011, **67**, 2794–2802.

17. Y. Xiang, A. Tong, P. Jin, and Y. Ju, *Org. Lett.*, 2006, **8**, 2863–2866.

18. X. Zeng, L. Dong, C. Wu, L. Mu, S.-F. Xue, and Z. Tao, *Sensors Actuators B Chem.*, 2009, **141**, 506–510.

19. X. Chen, M. J. Jou, H. Lee, S. Kou, J. Lim, S.-W. Nam, S. Park, K.-M. Kim, and J. Yoon, *Sensors Actuators B Chem.*, 2009, **137**, 597–602.

20. M. Zhao, X.-F. Yang, S. He, and L. Wang, *Sensors Actuators B Chem.*, 2009, **135**, 625–631.

21. Y. Zhou, F. Wang, Y. Kim, S.-J. Kim, and J. Yoon, *Org. Lett.*, 2009, **11**, 4442–4445.

22. Z. Xu, L. Zhang, R. Guo, T. Xiang, C. Wu, Z. Zheng, and F. Yang, *Sensors Actuators B Chem.*, 2011, **156**, 546–552.

23. Z. Xu, Y. Xiao, X. Qian, J. Cui, and D. Cui, *Org. Lett.*, 2005, **7**, 889–892.

24. J. Huang, Y. Xu, and X. Qian, *Dalt. Trans.*, 2009, 1761–1766.

25. Z. Xu, J. Pan, D. R. Spring, J. Cui, and J. Yoon, *Tetrahedron*, 2010, **66**, 1678–1683.

26. J. F. Zhang, Y. Zhou, J. Yoon, Y. Kim, S. J. Kim, and J. S. Kim, *Org. Lett.*, 2010, **12**, 3852–3855.

27. L. Zeng, E. W. Miller, A. Pralle, E. Y. Isacoff, and C. J. Chang, *J. Am. Chem. Soc.*, 2006, **128**, 10–11.

28. C.-Y. Chou, S.-R. Liu, and S.-P. Wu, *Analyst*, 2013, **138**, 3264–3270.

29. M. H. Kim, J. H. Noh, S. Kim, S. Ahn, and S.-K. Chang, *Dye. Pigment.*, 2009, **82**, 341–346.

30. R. Martínez, F. Zapata, A. Caballero, A. Espinosa, A. Tárraga, and P. Molina, *Org. Lett.*, 2006, **8**, 3235–3238.

31. W.-C. Lin, C.-Y. Wu, Z.-H. Liu, C.-Y. Lin, and Y.-P. Yen, *Talanta*, 2010, **81**, 1209–1215.

32. Y. Chen and J. Jiang, *Org. Biomol. Chem.*, 2012, **10**, 4782–4787.

33. H. Y. Lee, H. Son, J. M. Lim, J. Oh, D. Kang, W. S. Han, and J. H. Jung, *Analyst*, 2010, **135**, 2022–2027.

34. K. Sreenath, T. G. Thomas, and K. R. Gopidas, *Org. Lett.*, 2011, **13**, 1134–1137.

35. E. Sanna, L. Martínez, C. Rotger, S. Blasco, J. González, E. García-España, and A. Costa, *Org. Lett.*, 2010, **12**, 3840–3843.

36. M. R. Ajayakumar, D. Asthana, and P. Mukhopadhyay, *Org. Lett.*, 2012, **14**, 4822–4825.

37. O. García-Beltrán, B. K. Cassels, C. Pérez, N. Mena, M. T. Núñez, N. P. Martínez, P. Pavez, and M. E. Aliaga, *Sensors (Basel).*, 2014, **14**, 1358–71.

38. M. Shellaiah, Y.-H. Wu, A. Singh, M. V Ramakrishnam Raju, and H.-C. Lin, *J. Mater. Chem. A*, 2013, **1**, 1310–1318.

39. L. Qu, C. Yin, F. Huo, J. Chao, Y. Zhang, and F. Cheng, *Sensors Actuators B Chem.*, 2014, **191**, 158–164.

40. Z. Chen, L. Wang, G. Zou, J. Tang, X. Cai, M. Teng, and L. Chen, *Spectrochim. Acta. A. Mol. Biomol. Spectrosc.*, 2013, **105**, 57–61.

41. S. Sarkar, S. Roy, A. Sikdar, R. N. Saha, and S. S. Panja, *Analyst*, 2013, **138**, 7119–26.

42. K. B. Kim, H. Kim, E. J. Song, S. Kim, I. Noh, and C. Kim, *Dalton Trans.*, 2013, **42**, 16569–77.

43. H. Ye, F. Ge, Y.-M. Zhou, J.-T. Liu, and B.-X. Zhao, *Spectrochim. Acta. A. Mol. Biomol. Spectrosc.*, 2013, **112**, 132–8.

44. H. M. Chawla and W. A. Siddiqui, 2012, **1**, 39–44.